Electronic Supplementary Information

for

Room-Temperature Electrochemical Reduction of Epitaxial Bi_2O_3 Films to Epitaxial Bi Films

Zhen He,[*ab] *Jakub A. Koza,*[b] *Ying-Chau Liu,*[b] *Qingzhi Chen*[b] *and Jay A. Switzer*[b]

[a]College of Chemistry and Chemical Engineering, Central South University, Changsha, Hunan 410083, P. R. China

[b]Department of Chemistry and Graduate Center for Materials Research, Missouri University of Science and Technology, Rolla, Missouri 65401-1170, United States

[*]To whom correspondence should be addressed. E-mail: zhenhe@csu.edu.cn

This file includes:

1. *Experimental*

Electrochemical Reduction of Predeposited Bi_2O_3 Films to Bi Films. All electrochemical experiments were performed in a three-electrode set-up consisting of a Au electrode (an Au(111) single crystal or a polycrystalline Au electrode), a Ag/AgCl reference electrode (saturated with KCl), and a Pt mesh counter electrode. Epitaxial δ-Bi_2O_3 thin films were electrodeposited onto an Au (111) single crystal, and onto a polycrystalline Au electrode from a stirred solution containing 0.1 M $Bi(NO_3)_3 \cdot 5H_2O$, 0.25 M L-tartaric acid, and 2.5 M KOH at 65 °C by applying a constant anodic current density of 5 mA/cm^2 for 5000 seconds using a Brinkmann PGSTAT 30 Autolab potentiostat.[S1,S2] The predeposited δ-Bi_2O_3 thin films on Au substrates were electrochemically reduced to Bi thin films in 2 M NaOH at room-temperature by applying a constant potential of -0.8 V vs. Ag/AgCl for about 5200 seconds.

X-ray Diffraction Characterization. The XRD characterization of the electrodeposited epitaxial δ-Bi_2O_3 thin films and the Bi thin films after reduction were carried out on a high-resolution Philips X-Pert MRD X-ray diffractometer with a CuKα1 radiation source (λ = 0.154056 nm). The θ-2θ scans were obtained using the line focus mode with a hybrid monochromator consisting of a Göbel X-ray mirror and a Ge[220] two-bounce, two-crystal monochromator as the primary optic and a 0.18° thin film collimator as the secondary optic. The pole figure analysis was obtained in the point focus mode using a 2 mm × 2 mm crossed slit collimator with a Ni filter as the primary optic and a 0.27° parallel plate collimator with a flat graphite monochromator as the secondary optic. Pole figures were run by first setting the diffraction angle, 2θ, for a plane that was not parallel with the geometric surface of the film. Then the tilt angle, χ, was adjusted from 0 to 90° with an interval of 3°. The azimuthal angle at each tilt angle was rotated from φ = 0 to 360° with an interval of 3°.

X-ray Photoelectron Spectroscopy. The X-ray photoelectron spectra (XPS) of the predeposited Bi_2O_3 film and the Bi film after reduction were obtained in a Kratos AXIS 165 spectrometer using monochromatic AlKα radiation energy of 1486.6 eV. The Bi_2O_3 and Bi samples for the XPS investigation were as-prepared without any post surface treatment such as sputter profiling. All the binding energies in the spectra were referenced to the C 1s peak at 284.8 eV of the surface adventitious carbon.

Scanning Electron Microscopy and Energy Dispersive Spectroscopy. The surface morphologies of the Bi films after reduction were studied by a Hitachi S-4700 field-emission scanning electron microscope (FE-SEM) at an accelerating voltage of 15 kV. The energy dispersive spectroscopy (EDS) system equipped in the Hitachi S-4700 was used to analyze the chemical composition of the predeposited Bi_2O_3 film and the Bi film after reduction.

Magnetotransport Measurements. The magnetotransport property of the Bi thin film produced by direct electrochemical reduction of a δ-Bi_2O_3 thin film on Au(111) was measured in a Quantum Design Physical Property Measurement System (PPMS, San Diego, CA) with a resistivity option. Before the measurement, the Bi film was peeled off onto a nonconducting microscope glass slide using a commercial adhesive. Two silver wires were attached to the surface of the Bi film using pressed In contacts. The MR was measured in the perpendicular (P) geometry.[S3] That is, the magnetic field H is applied along the out-of-plane orientation of the Bi film and perpendicular to the direction of current flow. The MR was measured up to a field strength of 50 kOe.

References

[S1] Bohannan, E. W.; Jaynes, C. C.; Shumsky, M. G.; Barton, J. K.; Switzer, J. A. Low-temperature electrodeposition of the high-temperature cubic polymorph of bismuth(III) oxide. *Solid State Ionics* 2000, **131**, 97-107.

[S2] Switzer, J. A.; Shumsky, M. G.; Bohannan, E. W. Electrodeposited ceramic single crystals. *Science* 1999, **284**, 293-296.

[S3] Chien, C. L.; Yang, F. Y.; Liu, K.; Reich, D. H.; Searson, P. C. Very large magnetoresistance in electrodeposited single-crystal Bi thin films. *J. Appl. Phys.* 2000, **87**, 4659-4664.

2. *Volume expansion during the direct electrochemical reduction of δ-Bi_2O_3 to Bi.*

Bi has a rhombohedral lattice (space group $R\bar{3}m$) which can be superimposed onto a hexagonal lattice with a = b = 0.455 nm and c = 1.186 nm (as shown in Figs. S1a and S1b). In the hexagonal unit cell, the Bi

atoms are located at (0, 0, 0), (1/3, 2/3, 2/3) and (2/3, 1/3, 1/3), respectively. The volume of one hexagonal unit cell of Bi is calculated to be 0.2126 nm^3, which contains 10/3 Bi atoms. δ-Bi_2O_3 has a distorted fluorite structure (Fm3m, a = 5.525 Å) with Bi atoms at (0, 0, 0) and O atoms at 75% of (±1/4, ±1/4, ±1/4) as shown in Fig. S1c. One unit cell of δ-Bi_2O_3 has a volume of 0.1687 nm^3 and contains 4 Bi atoms. The reduction of one unit cell of δ-Bi_2O_3 could result in 1.2 hexagonal unit cells of Bi with a total volume of 0.2552 nm^3. Therefore, the direct electrochemical reduction of a δ-Bi_2O_3 thin film to a Bi thin film would theoretically result in about 51.3% volume expansion.

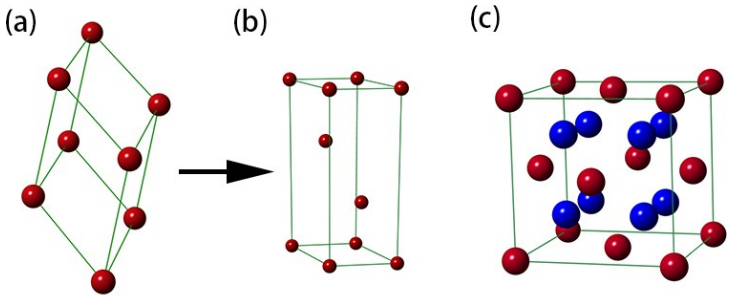

Fig. S1. Crystal structures of Bi in (a) rhombohedral lattice and (b) hexagonal lattice, and (c) crystal structure of δ-Bi_2O_3. The Bi atoms are shown as red spheres, whereas the O atoms are shown as blue spheres.

3. XPS and EDS Studies on the chemical state of Bi in predeposited δ-Bi_2O_3 film and the Bi film after reduction.

To study the change of oxidation state of Bi, XPS analyses were performed on the predeposited Bi_2O_3 film on Au(111) and the Bi film after reduction, as shown by the XPS survey scans in Fig. S2a. Note that the samples were not sputter profiled. For the Bi_2O_3 film, the Bi 4f spectrum (the black curve in Fig. S2b) shows two symmetric peaks centered at the binding energies (BEs) of 158.3 and 163.3 eV, respectively, which could be attributed to Bi $4f_{7/2}$ and Bi $4f_{5/2}$ levels. This spectrum matches well with the Bi 4f spectra of Bi_2O_3 in literature,[S4-S6] meaning that the Bi in the predeposited Bi_2O_3 film exists as Bi^{3+}. For the Bi film after reduction, two peaks centered at the BEs of 156.7 and 162.0 eV have emerged. These two peaks could be assigned to Bi $4f_{7/2}$ and Bi $4f_{5/2}$ levels for metallic Bi,[S7,S8] indicating that the Bi^{3+} in the Bi_2O_3 film has been reduced to Bi^0 after the electrochemical reduction process. In addition to the Bi 4f peaks from metallic Bi, there are two peaks centered at the BEs of 158.7 and 164 eV, respectively, which correspond to the Bi 4f peaks from the surface

oxide layer that is either unremoved after the reduction process or formed as the metallic Bi film is exposed to the oxygen in air. Please note that the samples for XPS are prepared and measured without any post surface treatment. It has been reported that the surfaces of metallic Bi are very sensitive to oxygen. An oxide layer could form on the surface immediately when the metallic Bi is exposed to oxygen even at 0.1 Torr and 145 K.[S8] We have mentioned in the main text that after the reduction process the loosely attached surface layer (due to the drastic volume and structure change during the reduction) consisting of metallic Bi and unreacted Bi_2O_3 could be removed (judging by naked eyes) by flushing with D. I. water or by using an adhesive tape. However, these simple treatments might not be able to completely remove the surface oxide layer. Since the XPS is a surface-sensitive technique, even a very small amount of oxide on the surface would be detected by the XPS. Compared to the XPS, the EDS could give a better idea of the overall composition of the films. The atomic percent of Bi and O in the Bi_2O_3 film and the Bi film after reduction measured by EDS are listed in Table S1. The EDS results show that the atomic ratio of Bi:O in the Bi_2O_3 film is close to 2:3, and the oxygen content in the reduced Bi film has decreased below the detection limit of the EDS. This also supports that the obtained film reduced from the predeposited Bi_2O_3 film is metallic Bi, although there might be a very thin layer of oxide (that is below the detection limit of the EDS) on the surface. The XPS and EDS results are consistent with the crystalline structure analysis by XRD (Fig. 2a), suggesting the formation of metallic, trigonal Bi film from the reduction of Bi_2O_3 film.

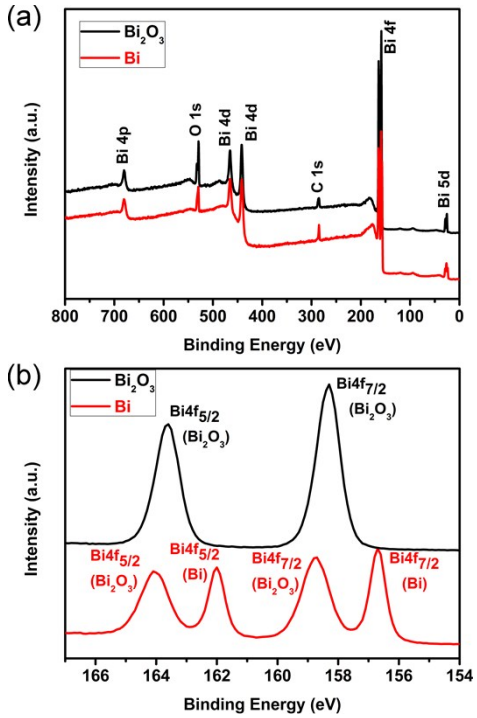

Fig. S2. X-ray photoelectron spectroscopy measurements of the predeposited Bi_2O_3 film and the Bi film after reduction. (a) Survey spectra of Bi_2O_3 film (black curve) and Bi film (red curve). (b) Bi 4f spectra of Bi_2O_3 film (black curve) and Bi film (red curve). All binding energies are calibrated for charging effects by referring to the C 1s peak at 284.8 eV.

Table S1. Atomic percent of Bi and O in the Bi_2O_3 film and the Bi film measured by EDS

	Bi atomic %	O atomic %
Bi_2O_3 film	40.70 ± 0.93	59.30 ± 0.93
Bi film	100%	below detection limit

References

[S4] Barreca, D.; Morazzoni, F.; Rizzi, G. A.; Scotti, R.; Tondello, E. Molecular oxygen interaction with Bi_2O_3: a spectroscopic and spectromagnetic investigation. *Phys. Chem. Chem. Phys.* 2001, **3**, 1743-1749.

[S5] Chen, R.; Shen, Z. –R.; Wang, H.; Zhou, H. –J.; Liu, Y. –P.; Ding, D. –T.; Chen, T. -H. Fabrication of mesh-like bismuth oxide single crystalline nanoflakes and their visible light photocatalytic activity. *J. Alloys Compd* 2011, **509**, 2588-2596.

[S6] Bian, Z. F.; Zhu, S. H.; Wang, Y.; Cao, X. F.; Qian, H. X.; Li, J. Self-assembly of active Bi_2O_3/TiO_2

visible photocatalyst with ordered mesoporous structure and highly crystallized anatase. *J. Phys. Chem. C* 2008, **112**, 6258.

[S7] Nascimento, V. B.; de Carvalho, V. E.; Paniago, R.; Soares, E. A.; Ladeira, L. O.; Pfannes, H. D. XPS and EELS study of the bismuth selenide. *J. Electron. Spectrosc.* 1999, **104**, 99-107.

[S8] Joyner, R. W.; Roberts, M. W.; Singh-Boparai, S. P. X-ray induced effects during the oxidation of Bi(0001). *Surf. Sci.* 1981, **104**, L199-L203.

4. Determination of the epitaxial relationships between the predeposited δ-Bi_2O_3 film and Au(111) substrate.

The in-plane orientations of the predeposited Bi_2O_3 film on Au(111) were measured by the X-ray pole figures as shown in Fig. 2b in the main text (also in Fig. S3g below). The in-plane orientations of the Bi_2O_3 film could be solved by comparing the measured X-ray pole figure with the corresponding stereographic projection generated using CaRIne 3.1 software. A stereographic projection is a plot which shows the angular relationships of the faces in the crystal based on its crystallographic structure. Single domain of Bi_2O_3(111)

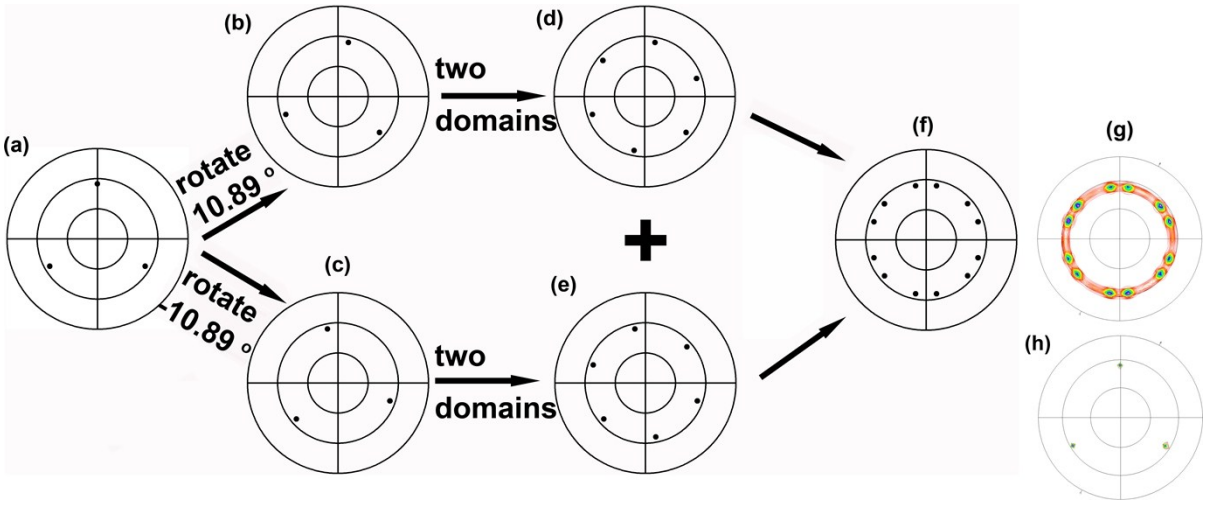

Fig. S3. Comparison of the calculated δ-Bi_2O_3 stereographic projections with the measured δ-Bi_2O_3 pole figure. (a) Bi_2O_3(111) stereographic projection probing the Bi_2O_3(200) type reflections. (b) Bi_2O_3(111) stereographic projection probing the Bi_2O_3(200) type reflections with the domain of Bi_2O_3 rotating 10.9° clockwise relative to the Au(111) substrate. (c) Bi_2O_3(111) stereographic projection probing the Bi_2O_3(200) type reflections with the domain of Bi_2O_3 rotating 10.9° counter-clockwise relative to the Au(111) substrate. (d) Overlapping of two antiparalleled domains of Bi_2O_3(111) stereographic projections in (b). (e) Overlapping of two antiparalleled domains of Bi_2O_3(111) stereographic projections in (c). (f) Overlapping of the two Bi_2O_3 stereographic projections in (d) and (e). (g) The measured (200) pole figure of the Bi_2O_3(111) film on Au(111). (h) The measured (311) pole figure of the Au(111) substrate.

stereographic projection probing Bi_2O_3(200) type reflections is shown in Fig. S3a. It shows an expected three-fold symmetry with three equally spaced ($\Delta\varphi$ = 120°) peaks appearing at a tilt angle, χ, of 54.7°, which matches with the interplanar angle between the {111} and {200} planes of Bi_2O_3. However, the measured (200) pole figure of Bi_2O_3(111) on Au(111) shows totally twelve diffraction peaks at the tilt angle of 54.7°, as shown in Fig. S3g. This indicates there are totally four domains of Bi_2O_3. Besides, the domains of Bi_2O_3 rotates about ±10.9° in-plane relative to the Au substrate by comparing the measured pole figures of Bi_2O_3 and the Au(111) substrate (in Fig. S3g and S3e, respectively). According the these analyses, the origin of the four domains of Bi_2O_3 in the measured (200) pole figure of the Bi_2O_3(111) on Au(111) could be explained as follows. The single domain of Bi_2O_3(111) rotates ±10.9° in-plane relative to the Au substrate as shown in Figs. S3b and S3c. Each of these rotated domains of Bi_2O_3(111) has an antiparalleled domain, as shown in Figs. S3d and S3e. Overall, there are totally four domains of Bi_2O_3(111) and twelve diffraction peaks in the stereographic projection in Fig. S3f, perfectly matching with the measured Bi_2O_3 pole figure (in Fig. S3g). Therefore, the epitaxial relationships between the four domains of Bi_2O_3 film and the Au(111) substrate are $Bi_2O_3(111)[2\bar{1}\,\bar{1}]||Au(111)[3\bar{2}\,\bar{1}]$, $Bi_2O_3(111)[\,\bar{2}\,11]||Au(111)[3\bar{2}\,\bar{1}]$, $Bi_2O_3(111)[2\bar{1}\,\bar{1}]||Au(111)[3\bar{1}\,\bar{2}]$ and $Bi_2O_3(111)\,[\,\bar{2}\,11]||Au(111)[3\bar{1}\,\bar{2}]$.

5. Determination of the epitaxial relationships between the Bi film after reduction and Au(111) substrate.

The in-plane orientations of the Bi film after reduction on Au(111) were measured by the X-ray pole figures as shown in Fig. 2c in the main text (also in Fig. S4e below). Single domain of Bi(012) stereographic projection probing Bi(116) type reflections is shown in Fig. S4a, which shows two diffraction peaks at tilt angles of about 27.0°, 65.3°, and 86.8°, respectively. The diffraction peaks at the tilt angle of 27.0º and 65.3° are azimuthally separated by about 92.4°, whereas the diffraction peaks at the tilt angle of 86.8° are azimuthally separated by about 38.4°. However, the measured (116) pole figure of Bi(012) on Au(111) has twelve diffraction peaks at each of these tilt angles. This indicates that there are six domains of Bi(112) on Au(111), which are azimuthally separated by 60.0°. The overlapping of six domains of Bi(012) stereographic

projections that are azimuthally spaced by 60° is shown in Fig. S4b. Besides, the three more diffraction peaks at the tilt angle of about 35.3° in the measured Bi(116) pole figure (Fig. S4e) arise from the Au(111) substrate. Because the 2θ values of Au(220) (about 64.6°) and Bi(116) (about 62.2°) are close, the low-angle tail of the Au(220) peak overlaps with the Bi(116) peak. Thus, when the 2θ angle is set to 64.6° to measure the Bi(116) pole figure, it is similar to the measurement of Au(220) pole figure. An Au(111) stereographic projection probing Au(220) type reflections is shown in Fig. S4c. When the Au(111) stereographic projection in Fig. S4c is overlapped with the six domains of Bi(012) stereographic projections in Fig. S4b, the resulted stereographic projection in Fig. S4d matches perfectly with the measured Bi(116) pole figure (Fig. S4e). The in-plane orientations of the Bi film could be solved by comparing the measured X-ray pole figure with the corresponding stereographic projection using CaRIne 3.1 software. Therefore, the epitaxial relationships of the six domains of Bi(012) film on Au(111) are Bi(012)[01$\bar{1}$]||Au(111)[$\bar{1}$ $\bar{1}$2], Bi(012)[01$\bar{1}$]||Au(111)[11$\bar{2}$], Bi(012)[01$\bar{1}$]||Au(111)[1$\bar{2}$1], Bi(012)[01$\bar{1}$]||Au(111)[$\bar{1}$2$\bar{1}$], Bi(012)[01$\bar{1}$]||Au(111)[2$\bar{1}$ $\bar{1}$], Bi(012)[01$\bar{1}$]||Au(111)[$\bar{2}$11].

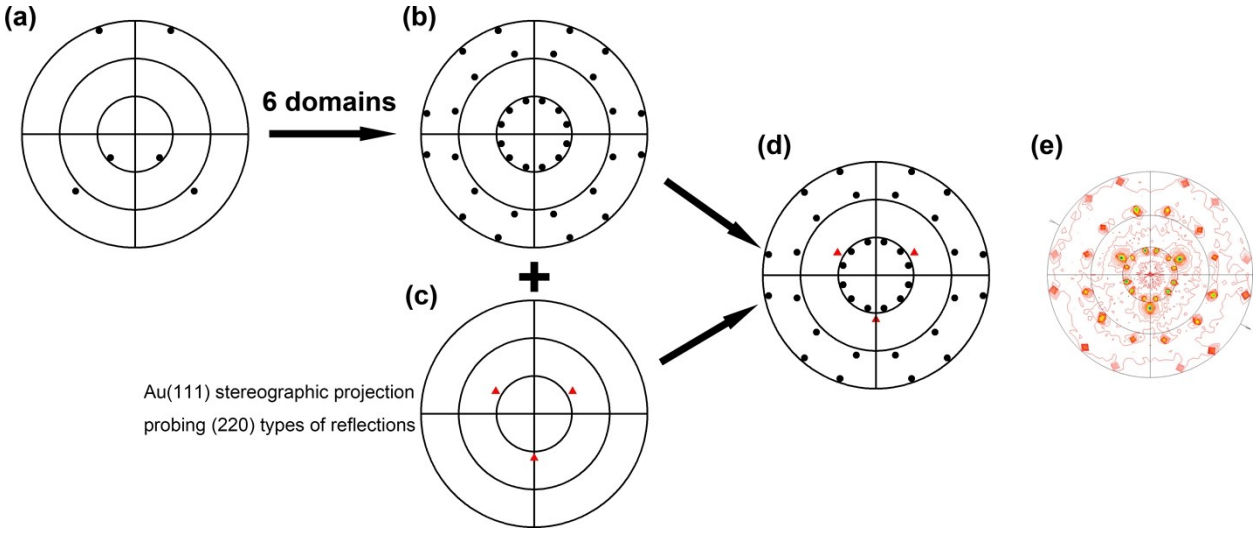

Fig. S4. Comparison of the calculated Bi stereographic projections with the measured Bi pole figure. (a) Bi(012) stereographic projection probing the (116) type reflections. (b) Overlapping of six domains of Bi(012) stereographic projections which are azimuthally spaced by 60°. (c) Au(111) stereographic projection probing the (220) type reflections. (d) Overlapping of the Bi(012) stereographic projection in (b) with the Au(111) stereographic projection in (c). (e) The measured (116) pole figure of Bi(012) on Au(111).